

Electronic Supplementary Information (ESI)

**Three-level Hierarchical Self-Assembly into Superhelical  
Nanostructures with Light-Switchable Helicity**

Huiya Li,<sup>a</sup> and Liang Chen<sup>\*b</sup>

*a International Collaborative Laboratory of 2D Materials for Optoelectronics Science and Technology of  
Ministry of Education, Institute of Microscale Optoelectronics, Shenzhen University, Shenzhen 518060,  
China.*

*b State Key Laboratory of Molecular Engineering of Polymers, Department of Macromolecular Science,  
Fudan University, Shanghai 200433, China.*

*E-mail: liangchen16@fudan.edu.cn*

## 1. Materials.

p-Nitrobenzoic acid (TCl, 99%), glucose (TCl), thionyl chloride (TCl, 99%), L-phenylalaninemethyl ester hydrochloride (Energy Chemical, 98%), D-phenylalaninemethyl ester hydrochloride (Energy Chemical, 98%), triethylamine (Energy Chemical, 99.5 %), sodium hydroxide (Energy Chemical, 97%), acetic acid (Energy Chemical, 99.5%), hydrochloric acid (TCl, 36~38%). All of the solvents, including ethanol, methanol, THF, dichloromethane, were purchased from Shanghai Chemical Ltd Co. Anhydrous  $\text{CH}_2\text{Cl}_2$  were purchased from Sigma and used without purification. Unless specially mentioned, all chemicals were used as received.

## 2. Methods.

**Nuclear Magnetic Resonance (NMR)** was taken by AVANCE III HD 400 MHz of Bruker BioSpin International for characterization of the  $^1\text{H}$  NMR and  $^{13}\text{C}$  NMR spectra of all the samples and used  $\text{CDCl}_3$  or  $d_6$ -DMSO as the solvents. **Matrix Assisted Laser Desorption Ionization Time-of-Flight Mass Spectroscopy (MALDI-TOF MS)** was used for characterization of the molecular weights of all the samples by an AB SCIEX 5800 system and used Trans-2-[3-(4-tert-Butylphenyl)-2-methyl-2-propenylidene] (DCTB) as the matrix. **Dynamic Light Scattering (DLS)** was used to determine the hydrodynamic diameters and distribution of the samples by a Malvern Zetasizer Nano ZS. The scattering angle is fixed on  $90^\circ$ . **UV-vis Spectroscopy (UV-vis)** was recorded by an Agilent Cary-60 UV-Vis spectroscopy. **Transmission Electron Microscopy (TEM)** was tested using a JEOL 2000 EX electron microscope operated at 200 kV. **Scanning Electron Microscope (SEM)** was performed on a Zeiss Gemini SEM500 electron microscope. Before observation the surface, samples were sputtered with a thin layer of Au for increasing the electrical conductivity. **Circular Dichroism (CD)** was recorded on a JASCO J-175 spectrometer. **Optical Microscope (OP)** was recorded on a Zeiss Axio Imager 2 metallographic microscope.

### 3. Synthetic Routes

The synthesis of Bis-L/D-phenylalanine-terminated azobenzene ( $F^L\text{Azo}F^L$  and  $F^D\text{Azo}F^D$ ) was performed in four steps, as shown in Figure S1.

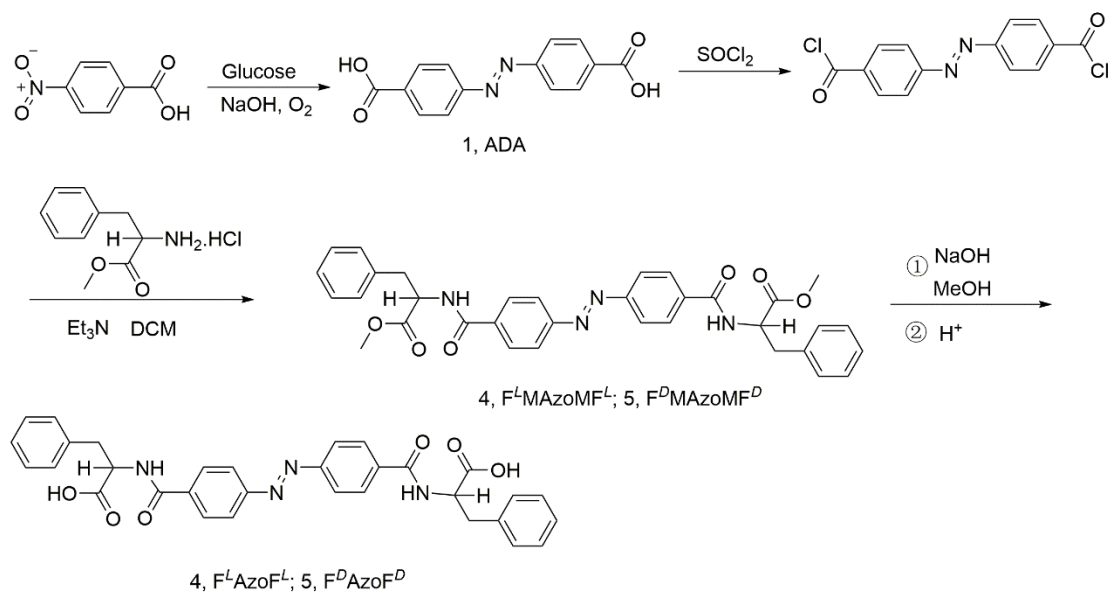


**Fig. S1** Synthetic route of the  $F^L\text{Azo}F^L$  and  $F^D\text{Azo}F^D$ .

**Step 1: Compound 2 (ADA).** The synthesis of azobenzene-4,4'-dicarboxylic acid (ADA) was performed according to a literature procedure.<sup>1</sup> 2 g of p-Nitrobenzoic acid and 6.7 g of sodium hydroxide were dissolved in 30 mL of distilled water at 50 °C. To this solution, a solution of 13.33 g of glucose dissolved in 20 mL distilled water was added dropwise, at the water bath temperature of 50 °C. The highly exothermic reaction results in the immediate formation of a dark brown solution. To this reaction mixture now a stream of air is passed with the help of an air pump. The reaction mixture was kept at 50 °C with constant air bubbling for 4-5 h and a chocolate brown precipitate was obtained. This was filtered and dissolved in distilled water and later acidified by drop wise addition of glacial acetic acid resulting in a light pink precipitate. This precipitate was filtered and washed with plenty of water and then dried in an oven. Yield is 68.8%. The <sup>1</sup>H NMR spectrum of ADA is shown in Figure S2. <sup>1</sup>H NMR (400 MHz, DMSO-*d*<sub>6</sub>) δ (ppm): 13.25 (s, 2H), 8.16 (d, 4), 8.10 (d, 4). The <sup>13</sup>C NMR spectrum of ADA is shown in Figure S3. <sup>13</sup>C NMR (400 MHz, DMSO-*d*<sub>6</sub>) δ (ppm): 166.59, 154.14, 133.36, 130.67, 122.81.

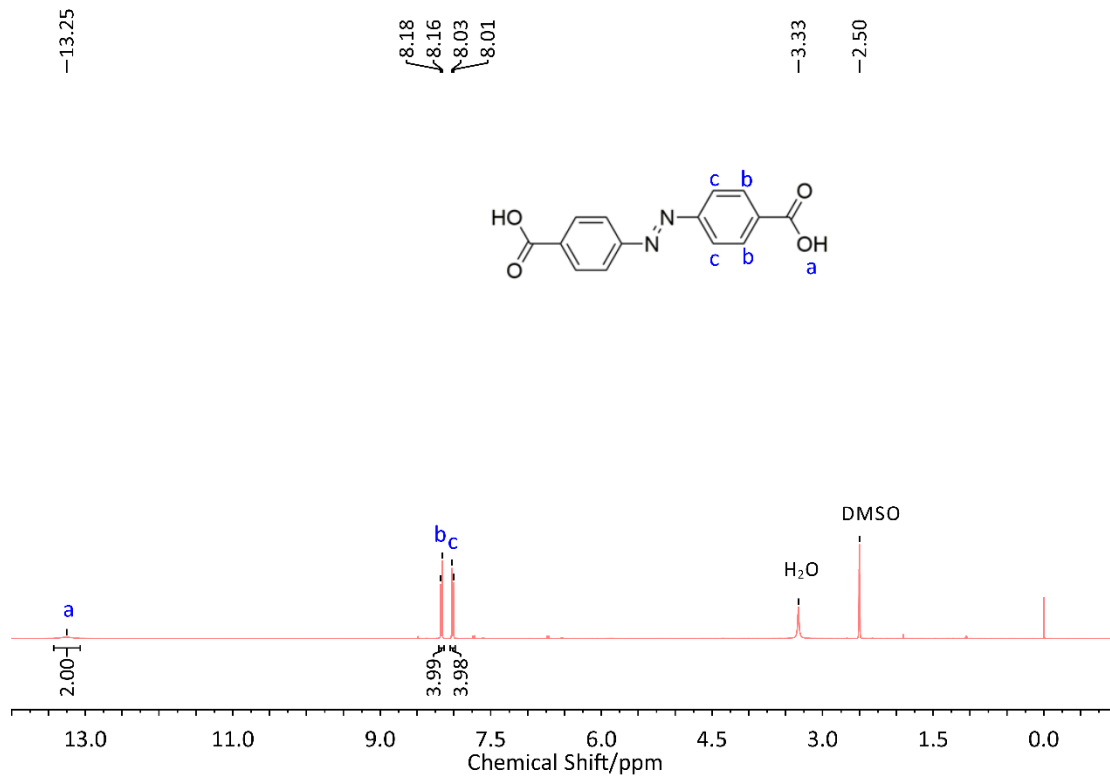


Fig. S2 <sup>1</sup>H NMR spectrum of ADA in DMSO-*d*<sub>6</sub>.

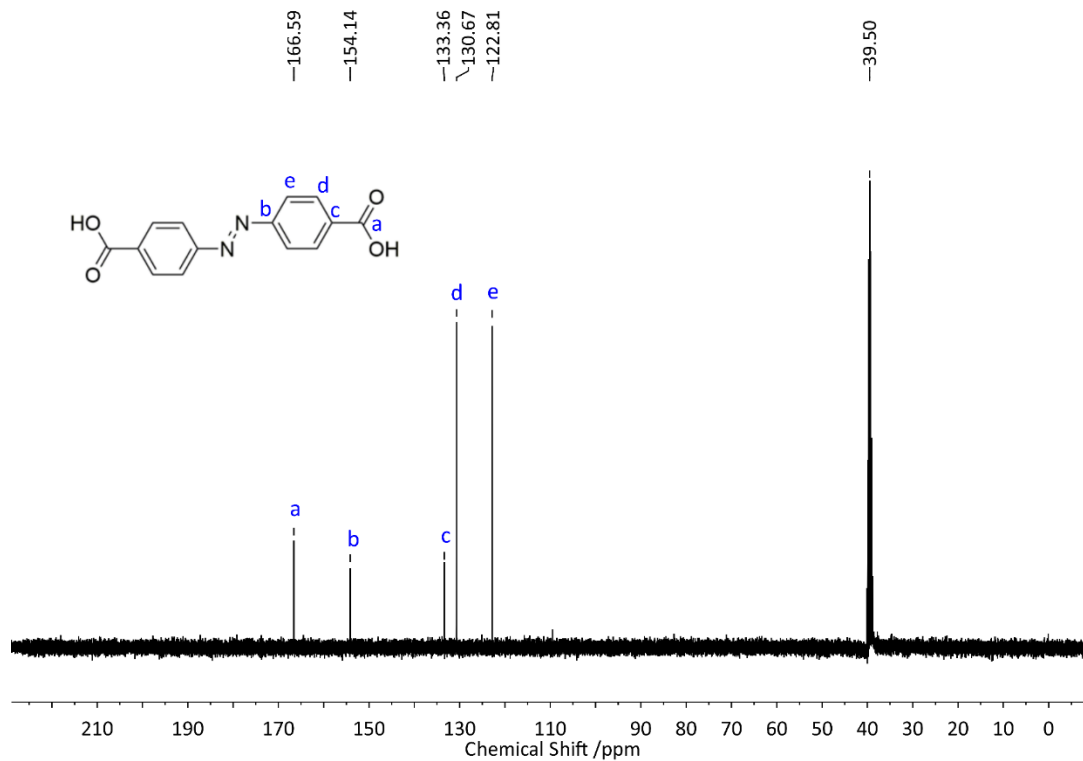
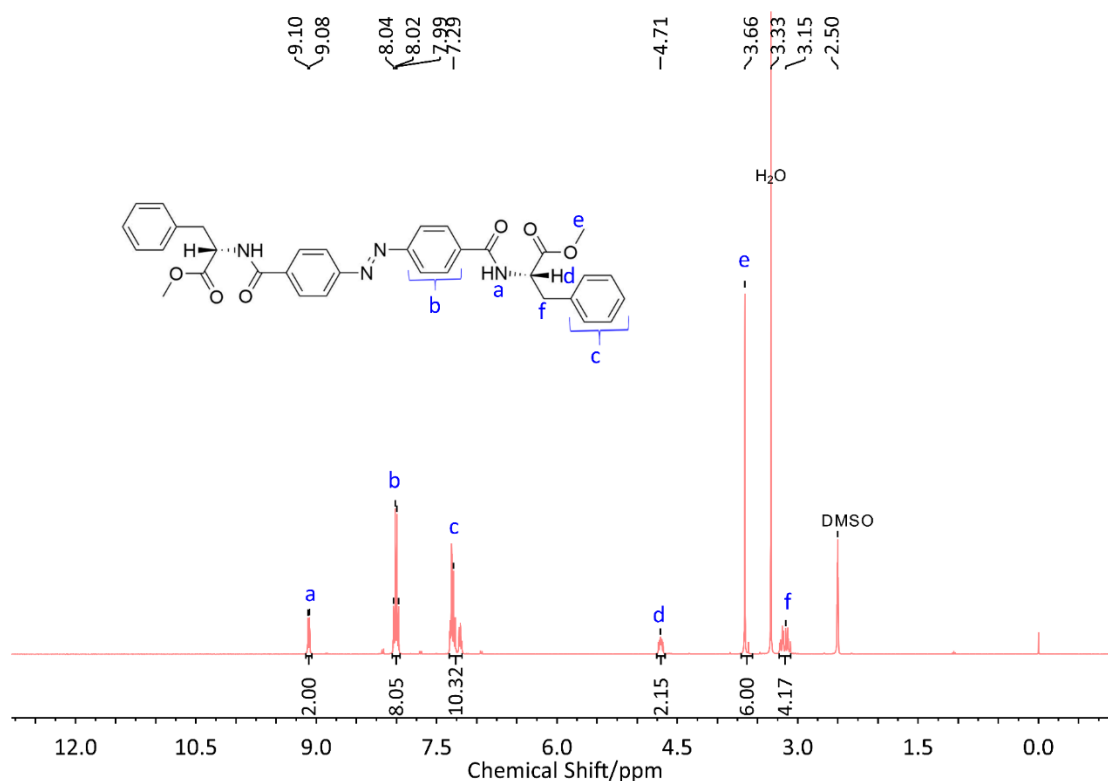
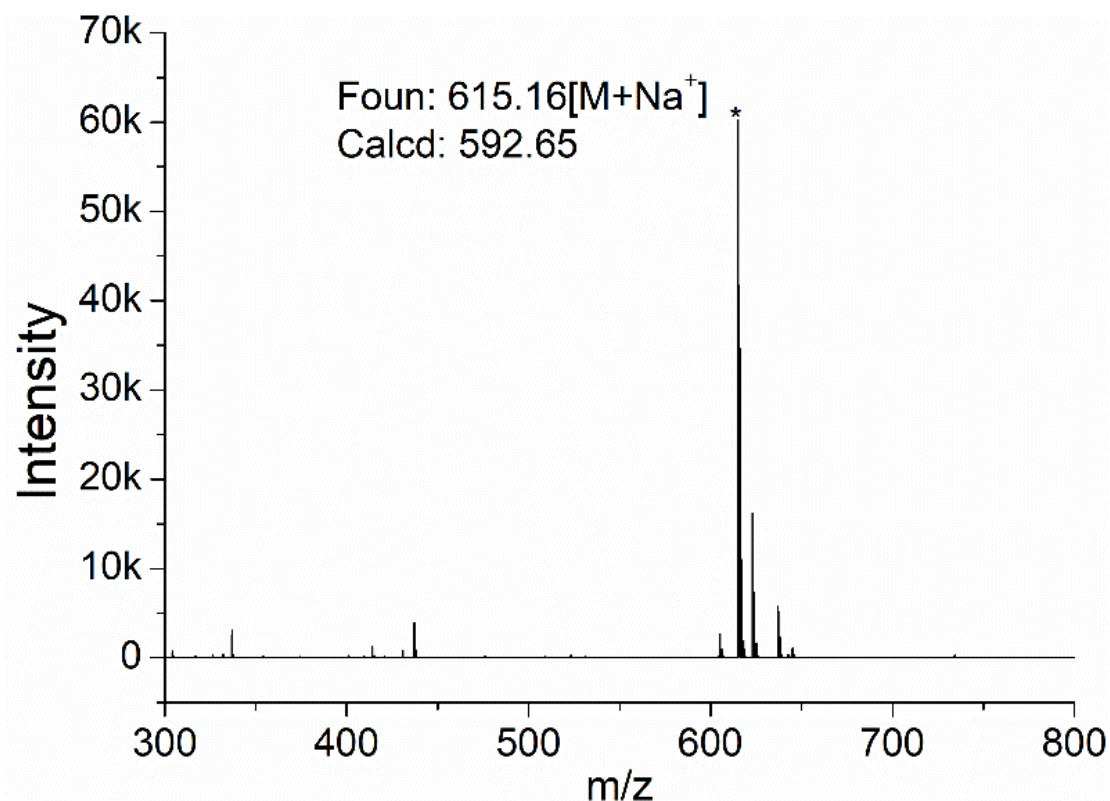


Fig. S3 <sup>13</sup>C NMR spectrum of ADA in DMSO-*d*<sub>6</sub>.

**Step 2 and step 3: Compound 2 ( $F^LMAzoMF^L$ ).** The synthesis of Bis-L-phenylalanine methyl ester-Terminated Azobenzene ( $F^LMAzoMF^L$ ) was performed according to the literature.<sup>2</sup> 2.70 g of ADA was added to 20 mL of thionyl chloride, and the mixture was stirred at 100 °C for 4 h. After removal of the solvent under reduced pressure, the residue was dissolved into 100 mL of dry dichloromethane and then was added dropwise to 100 mL dichloromethane solution containing 5.0 g of L-phenylalanine methyl ester hydrochloride and 3.6 mL of triethylamine in an ice-water bath. After completing the addition, the solution was stirred at room temperature overnight. All the solvents were evaporated upon vacuum, and the residue was subsequently dissolved in 100 mL of ethanol. After filtration, undissolved substance was collected. Yield is 81.4 %. The  $^1H$  NMR spectrum of  $F^LMAzoMF^L$  is shown in Figure S4.  $^1H$  NMR (400 MHz,  $DMSO-d_6$ )  $\delta$  (ppm): 13.25 (s, 2H), 9.08 (d, 2), 8.02 (q, 8), 7.29 (m, 10), 4.71 (m, 2), 3.66 (s, 6), 3.15 (m, 4). The MALDI-TOF mass spectrum of  $F^LMAzoMF^L$  is shown in Figure S5.  $m/z$  calcd for M  $C_{34}H_{32}N_4O_6$  592.65, found 615.16.



**Fig. S4**  $^1H$ NMR spectrum of  $F^LMAzoMF^L$  in  $DMSO-d_6$



**Fig. S5** The MALDI-TOF mass spectrum of  $F^L\text{MAzoMF}^L$ .

**Step4: Compound 4 ( $F^L\text{AzoF}^L$ ).** The synthesis of  $F^L\text{AzoF}^L$  was performed according to the literature.<sup>3</sup> For the hydrolysis, 10 mL aqueous NaOH (2 M) was added to a suspension of L-BPMA 3.00 g in 20 mL of methanol. The mixture was slowly brought back to room temperature and stirred for 24 h, and a clear solution was obtained. The solution was then acidified with 3M HCl to pH < 3, and a gel-like precipitate formed. The gel phase was filtered, washed with deionized water and finally dried in the vacuum oven to give  $F^L\text{AzoF}^L$ . Yield is 92.2%. The  $^1\text{H}$  NMR spectrum of  $F^L\text{AzoF}^L$  is shown in Figure S6.  $^1\text{H}$  NMR (400 MHz,  $\text{DMSO-}d_6$ )  $\delta$  (ppm): 12.86 (s, 2), 8.96 (d, 2), 8.01 (q, 8), 7.33 (m, 10), 4.66 (m, 2), 3.12 (m, 4). The  $^{13}\text{C}$  NMR spectrum of  $F^L\text{AzoF}^L$  is shown in Figure S7.  $^{13}\text{C}$  NMR (400 MHz,  $\text{DMSO-}d_6$ )  $\delta$  (ppm): 173.06, 165.54, 153.32, 138.12, 136.39, 129.06, 128.74, 128.23, 126.41, 122.58.

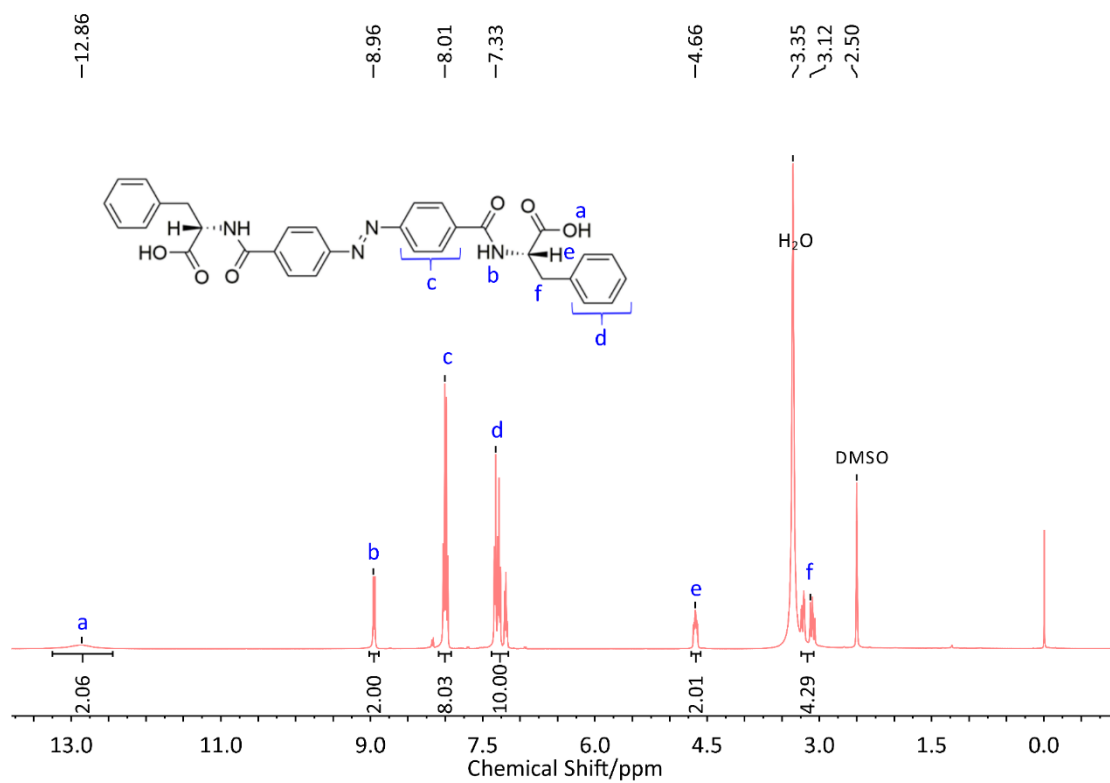


Fig. S6  $^1H$  NMR spectrum of  $F^L Azo F^L$  in  $DMSO-d_6$ .

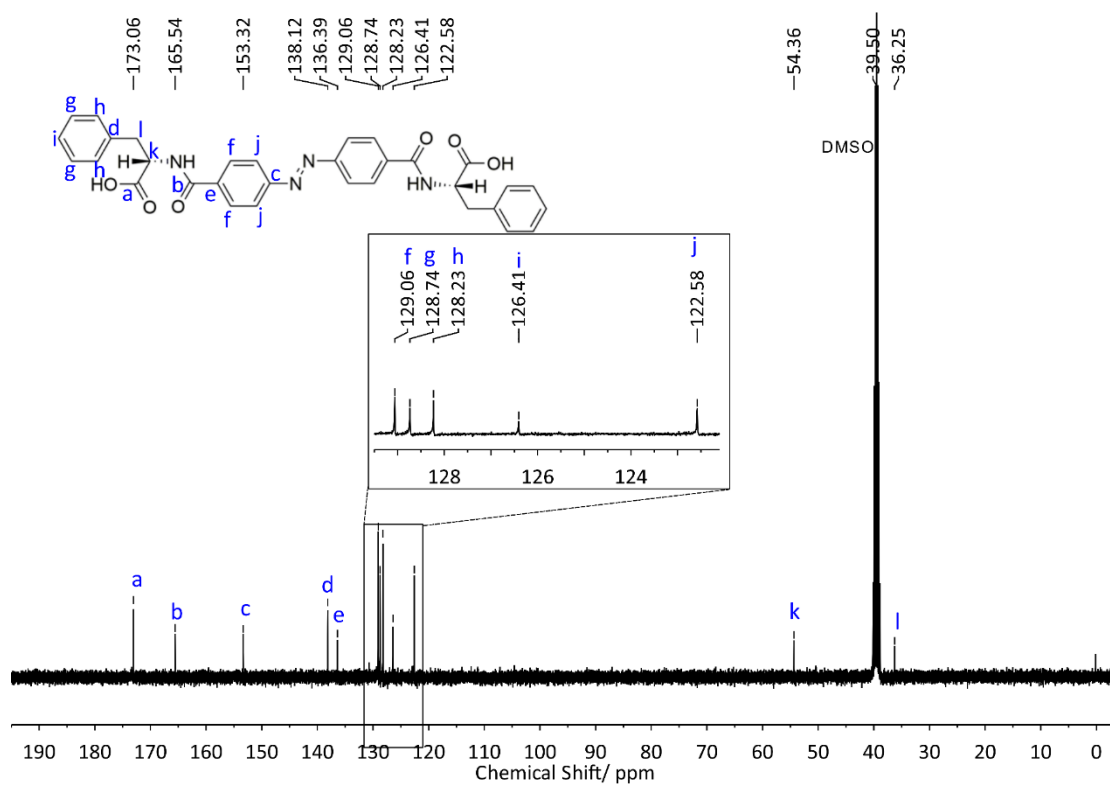
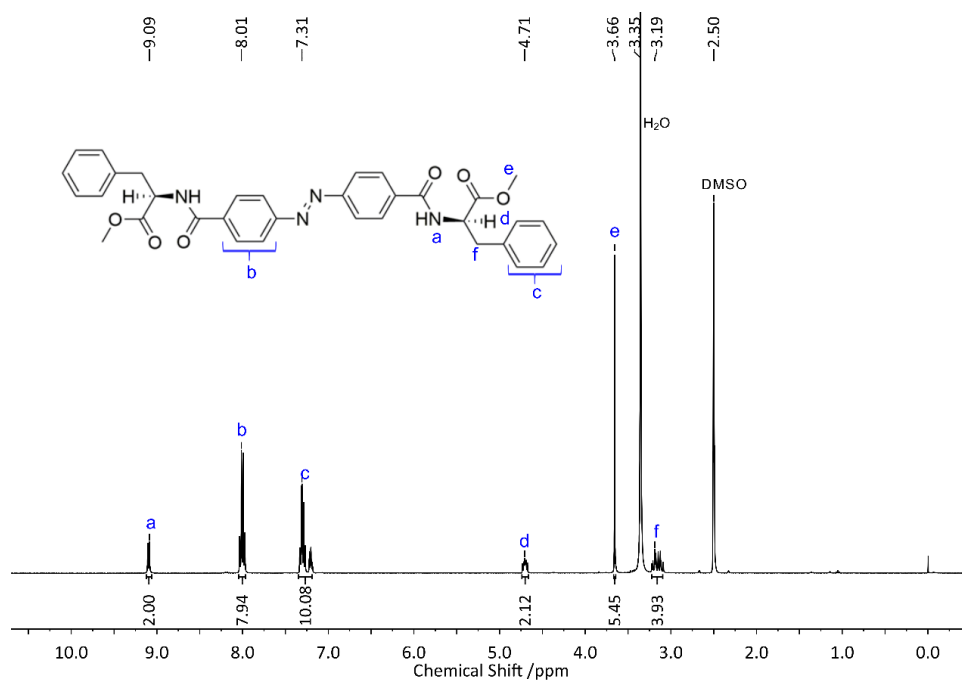
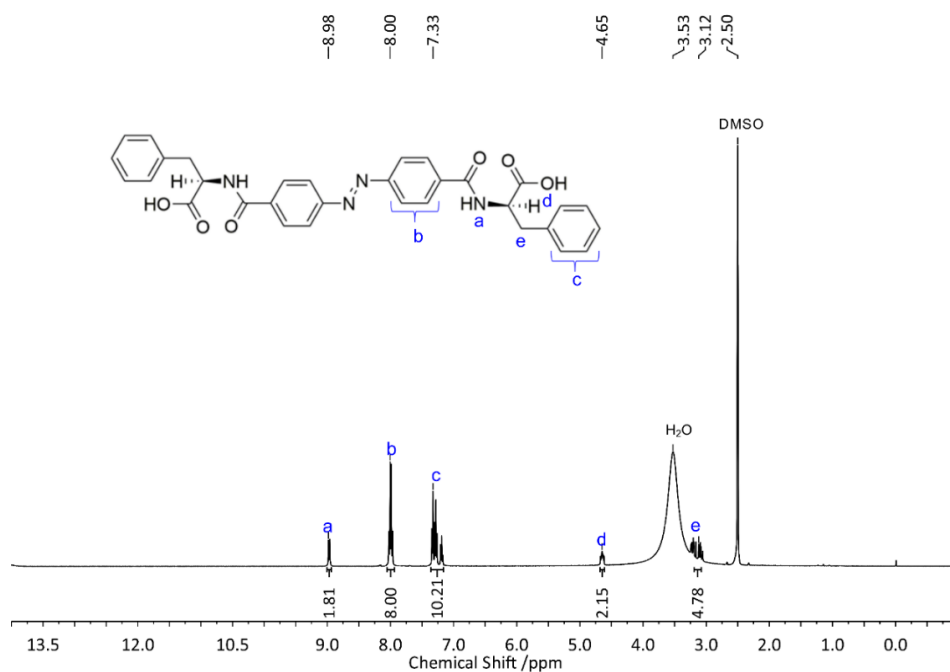


Fig. S7  $^{13}C$  NMR spectrum of  $F^L Azo F^L$  in  $DMSO-d_6$ .

**Compound 3 (D-BPMA) and Compound 5 ( $F^D$ Azo $F^D$ ).** The  $F^D$ Azo $F^D$  was prepared in a similar way. The  $^1\text{H}$  NMR spectrum of D-BPMA is shown in Figure S8.  $^1\text{H}$  NMR (400 MHz, DMSO- $d_6$ )  $\delta$  (ppm): 9.08 (d, 2), 8.01 (q, 8), 7.31 (m, 10), 4.71 (m, 2), 3.66 (s, 6), 3.19 (m, 4). The  $^1\text{H}$  NMR spectrum of  $F^D$ Azo $F^D$  is shown in Figure S8.  $^1\text{H}$  NMR (400 MHz, DMSO- $d_6$ )  $\delta$  (ppm): 8.98 (d, 2), 8.00 (q, 8), 7.33 (m, 10), 4.65 (m, 2), 3.12 (m, 4).



**Fig S8**  $^1\text{H}$ NMR spectrum of D-BPMA in DMSO- $d_6$ .



**Fig. S9**  $^1\text{H}$  NMR spectrum of  $F^D$ Azo $F^D$  in DMSO- $d_6$ .



#### 4 Additional experimental datas and figures

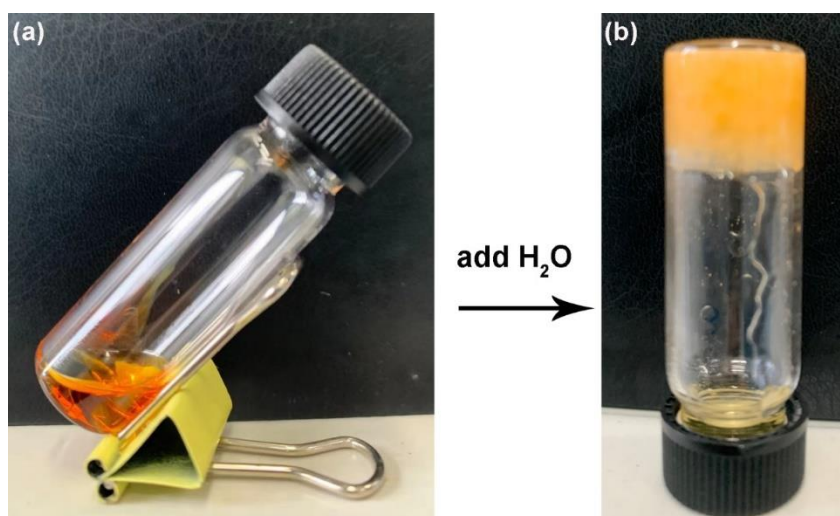


**Fig. S10** The photo images change of the self-assembly process. Simply, 3 mg of  $F^L\text{Azo}F^L$  was dissolved in 0.25 mL of THF to form an orange clear solution (Fig. S10a), then 1 mL of  $\text{H}_2\text{O}$  was injected into the above solution, after which the opaque self-supportive gel was formed (Fig. S10b).

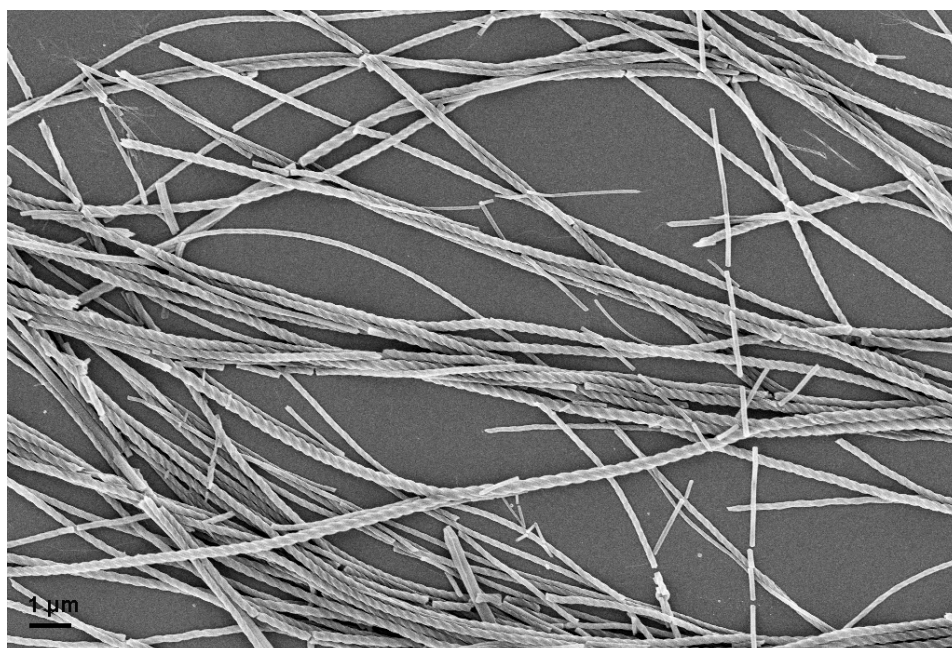


**Fig. S11** The large area SEM image of  $F^L\text{Azo}F^L$  superhelices.

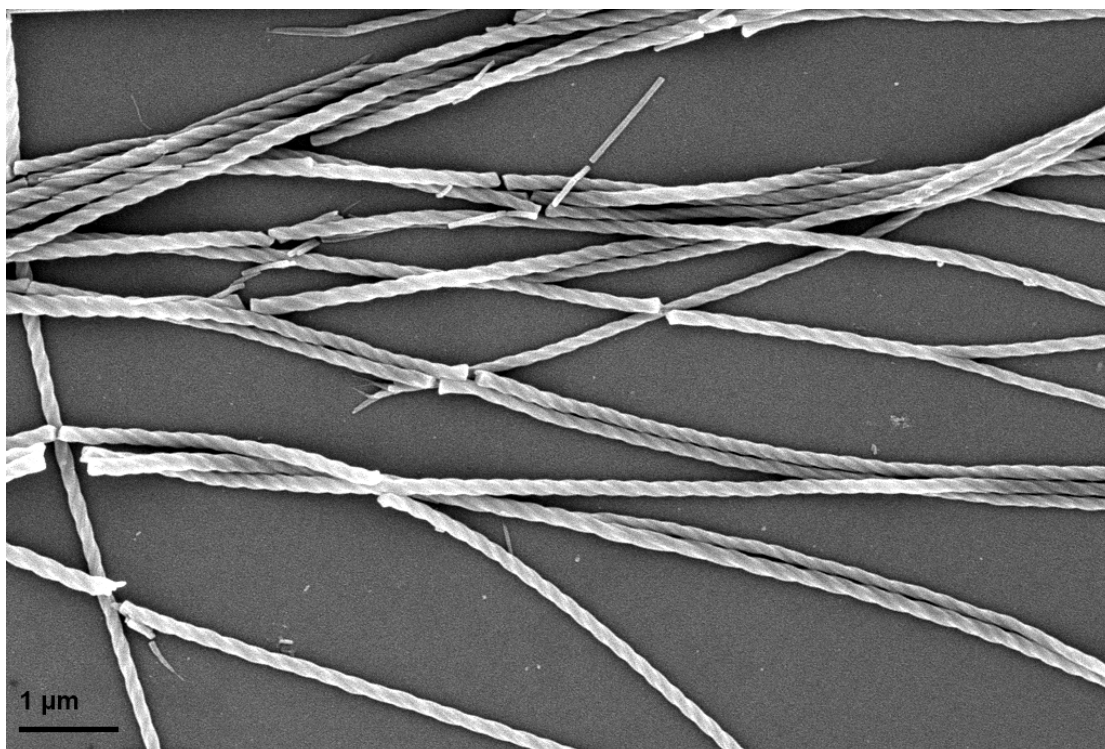


**Fig. S12** The large area SEM image of  $F^L AzoF^L$  superhelices.

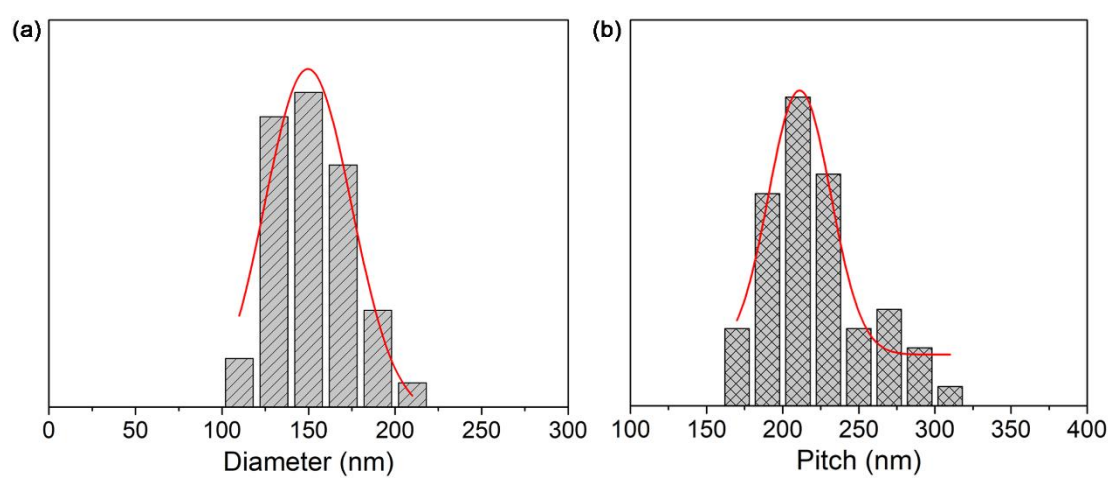


**Fig. S13** The diameter distribution (a) and pitch distribution (b) obtained from SEM images of  $F^L AzoF^L$  superhelices, which were analyzed by Nano Measurer software. The average diameter is  $152.9 \pm 21.8$  nm and the average helical pitch is  $222.72 \pm 31.92$  nm.

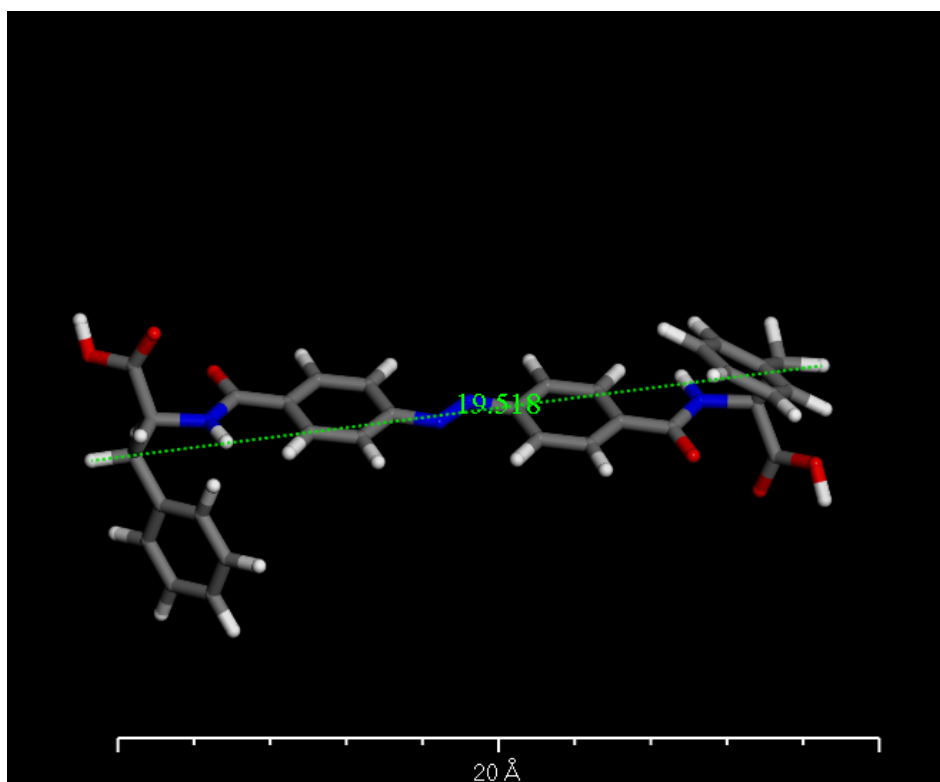


**Fig S14** Estimation of the length of a  $F^L Azo F^L$  molecule calculated with Materials Studio package. The length is around 1.95 nm.

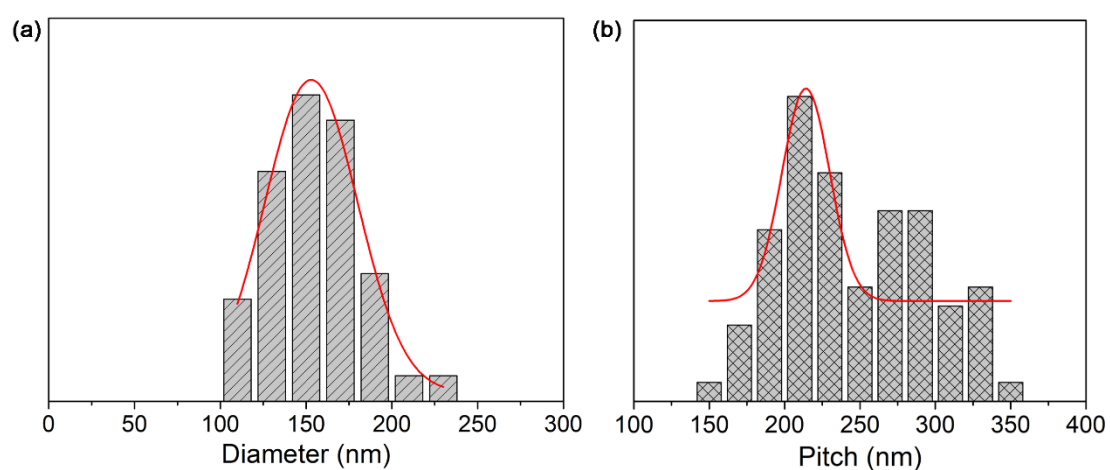


**Fig. S15** The diameter distribution (a) and pitch distribution (b) obtained from SEM images of  $F^D Azo F^D$  superhelices, which were analyzed by Nano Measurer software. The average diameter is  $155.2 \pm 26.8$  nm and the average helical pitch is  $245.72 \pm 48.87$  nm.



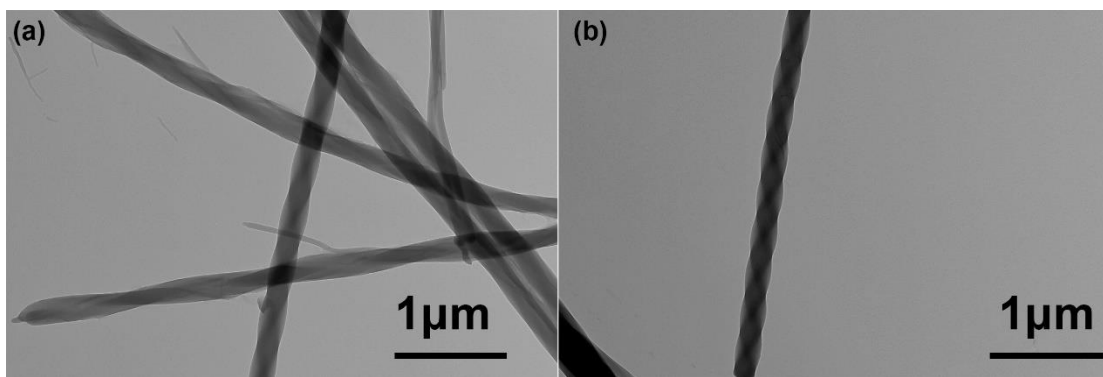


**Fig. S16** TEM images of the supramolecular  $F^L Azo F^L$  gels.

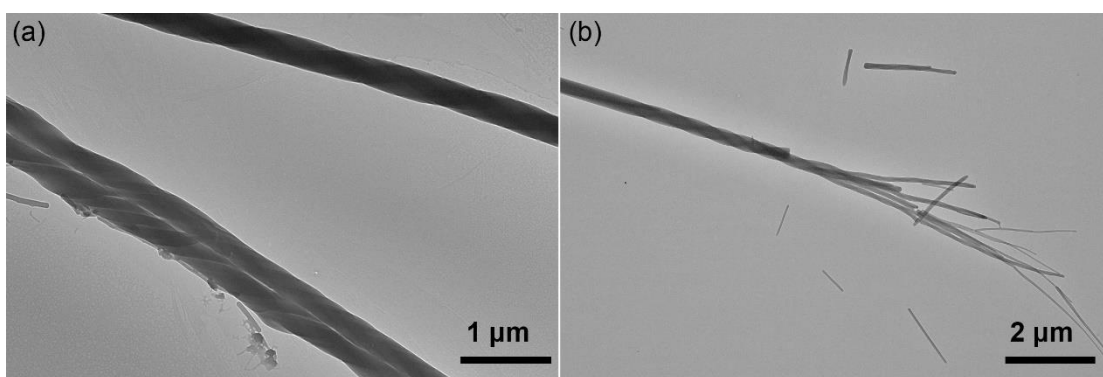


**Fig. S17** TEM images of the supramolecular  $F^D Azo F^D$  gels.

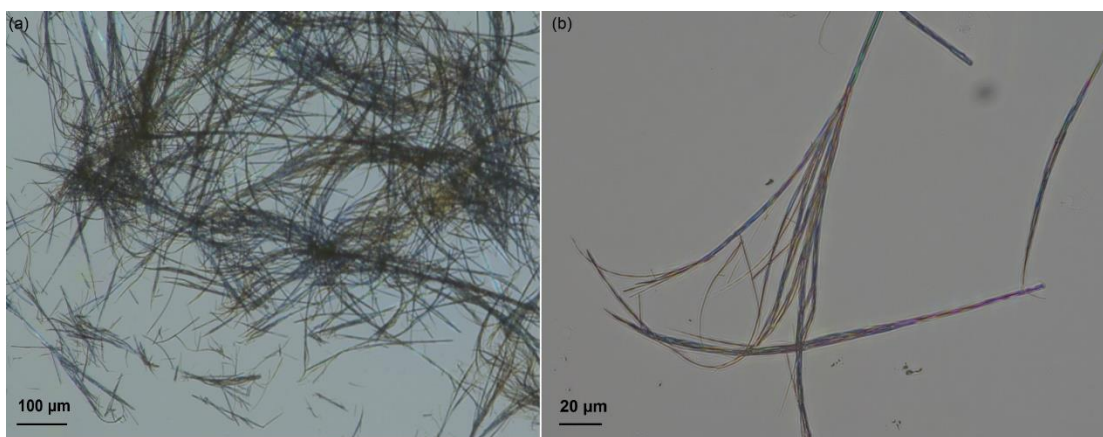


**Fig. S18** *In-situ* observe the superhelical nanofibers of  $F^L Azo F^L$  gels by using optical microscope.

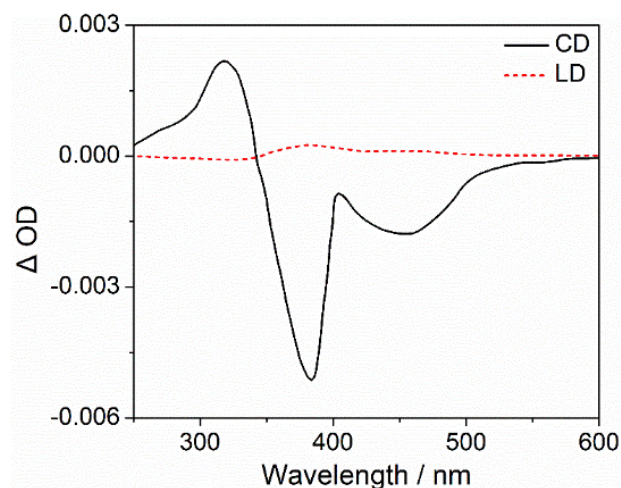


**Fig. S19** The CD spectra with the unit  $\Delta OD$  for comparison with the LD spectra of  $F^L AzoF^L$  gels. The contamination of CD by LD is quantitatively estimated about 0.92% according to the following semi-empirical equation: Contamination of CD by LD = LD \* 0.02 / CD observed, indicating that the LD contribution could be negligible in these gels.

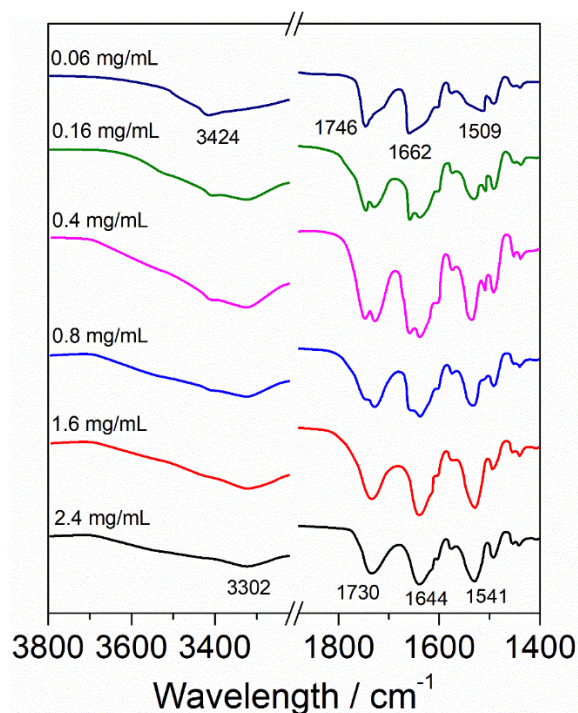


**Fig. S20** The concentration-dependent FTIR spectra of  $F^L AzoF^L$  in the mixed solution of THF and  $H_2O$  at the ratio of 1:4. The FTIR spectrum at low concentration of 0.06 mg/mL, in which no self-assembly occurred, showed absorption bands at 3442 ( $\nu_{N-H}$ , amide II), 1662 ( $\nu_{C=O}$ , amide I), 1509 ( $\delta_{N-H}$ , amide II)  $cm^{-1}$ , characteristic of non-hydrogen-bonded. With the concentration increasing, these peaks gradually shifted into 3302, 1644,

1541  $\text{cm}^{-1}$ , respectively, which are assigned to hydrogen-bonded amide groups<sup>[4-5]</sup>. These results indicate that  $F^L\text{Azo}F^L$  form intermolecular hydrogen bonds in the superhelical nanofibers. Moreover, the absorption peak at 1746  $\text{cm}^{-1}$  (free state), corresponding to C=O stretching vibration of carboxy groups, shifted into 1730  $\text{cm}^{-1}$  (gels state), indicate that the hydrogen bonds also occurred between carboxy groups.

[6]

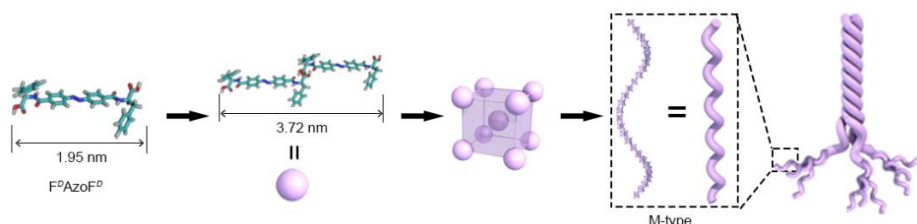


**Fig. S21** Proposed molecular stacking mechanism of  $F^D\text{Azo}F^D$  gels.

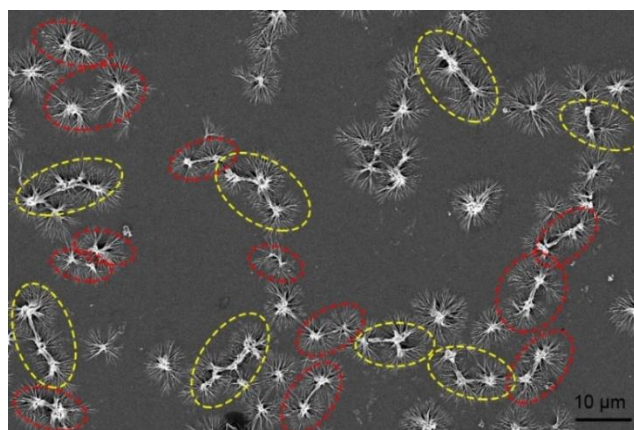


**Fig. S22** SEM image showing the formation of some dimers (red circle) and trimers (yellow circle) of the sea urchin-like superhelices at the solvent ratio of 1: 0.5.

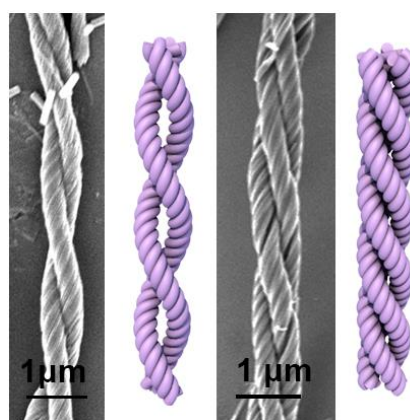


**Fig. S23** SEM images showing the formation of some more complex four-level hierarchical double superhelices and triple superhelices at the solvent ratio of 1: 6.



**Fig. S24** Keeping the solvent conditions unchanged (THF/H<sub>2</sub>O, 1/4, v/v), decreasing the concentration of F<sup>L</sup>AzoF<sup>L</sup> to 0.16 mg/mL led to the formation of needle-like aggregates.

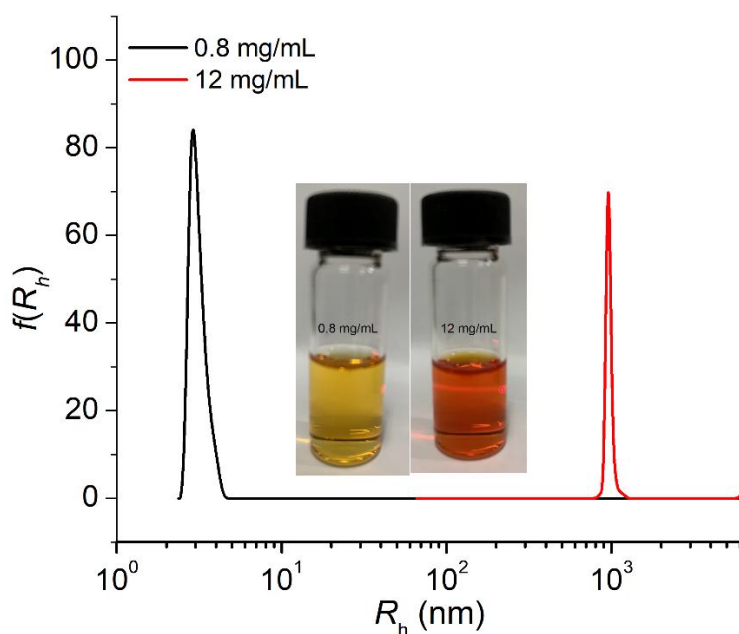


**Fig. S25** Dynamic laser scattering (DLS) and photo images showing the self-assembly behavior in pure THF at different F<sup>L</sup>AzoF<sup>L</sup> concentrations. Photo images show that an obvious Tyndall effect is found at high F<sup>L</sup>AzoF<sup>L</sup> concentration (12.0 mg/THF), while the F<sup>L</sup>AzoF<sup>L</sup> solution at low concentration (0.8 mg/THF) doesn't scatter light. DLS results show that the hydrodynamic radius at high F<sup>L</sup>AzoF<sup>L</sup> concentration is ~ 975.2 nm, while it is ~ 2.90 nm at low F<sup>L</sup>AzoF<sup>L</sup> concentration.



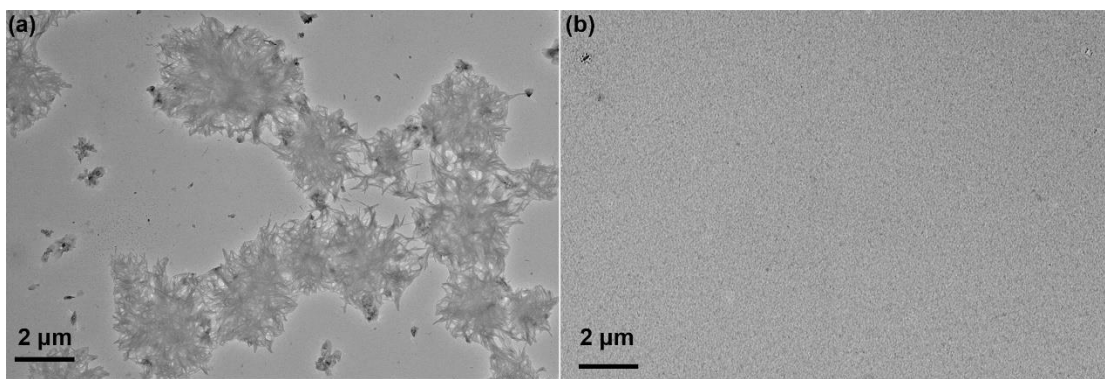


**Fig. S26** TEM images showing the self-assembly behavior in pure THF at different  $F^L AzoF^L$  concentrations. (a) 12 mg/mL; (b) 0.8 mg/mL.

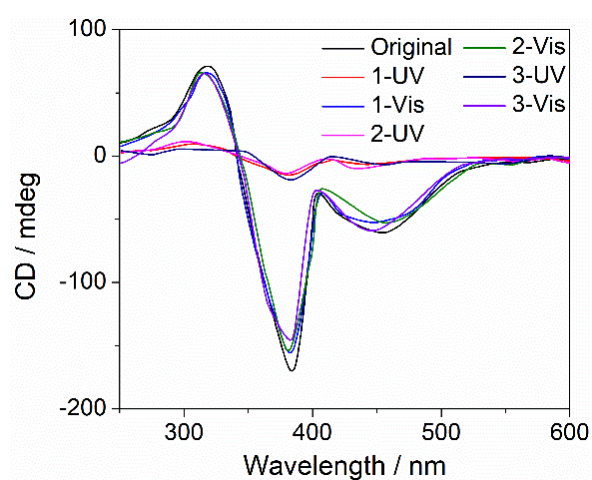


**Fig. S27** The CD spectra of  $F^L AzoF^L$  superhelical nanofiber gel in three cycles of alternating 365nm and 440 nm light irradiation.

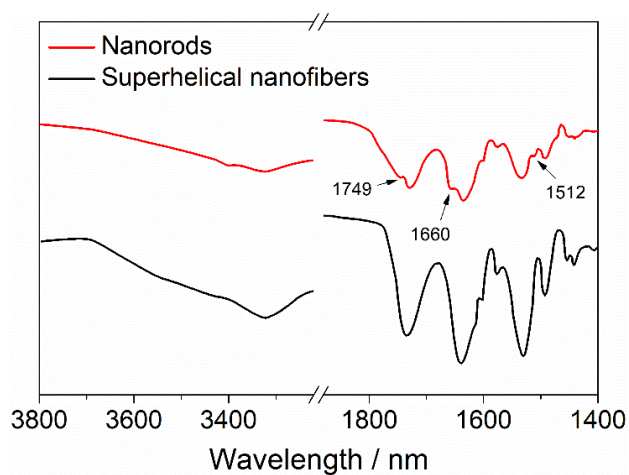


**Fig. 28** FTIR spectra of  $F^L AzoF^L$  in superhelical nanofibers and in nanorods.



## 5 References

- [1] Hong, Y.; Gao, Z.; Chen, M.; Hao, J.; Dong, S. Metal-Organic Gels of Catechol-Based Ligands with Ni (II) Acetate for Dye Adsorption. *Langmuir* **2018**, *34*, 9435-9441.
- [2] Lim, C.; Li, X.; Li, Y.; Drew, K.; Hernandez, J.; Tang, Z.; Baev, A.; Kuzmin, A.; Knecht, M.; Walsh, T.; Swihart, M.; Ågren, H.; Prasad, P. Plasmon-enhanced two-photon-induced isomerization for highly-localized light-based actuation of inorganic/organic interfaces. *Nanoscale* **2016**, *8*, 4194-4202.
- [3] Liu, G.; Liu, J.; Feng, C.; Zhao, Y. Unexpected right-handed helical nanostructures co-assembled from L-phenylalanine derivatives and achiral bipyridines. *Chem. Sci.* **2017**, *8*, 1769.1775.
- [4] Duan, P.; Li, Y.; Li, L.; Deng, J.; Liu, M. Multiresponsive chiroptical switch of an azobenzene-containing lipid: Solvent, temperature, and photoregulated supramolecular chirality. *J. Phys. Chem. B* **2011**, *115*, 3322-3329
- [5] Suzuki, M.; Yumoto, M.; Kimura, M.; Shirai, H.; Hanabus, K. New low-molecular-weight hydrogelators based on L-lysine with positively charged pendant chain. *New J. Chem.* **2002**, *26*, 817-818
- [6] Liu, G.; Zhou, C.; Teo, W.; Qian, C.; Zhao, Y. Self-Sorting Double-Network Hydrogels with Tunable Supramolecular Handedness and Mechanical Properties. *Angew. Chem. Int. Ed.* **2019**, *58*, 9366-9372